5

How to Make FRET Biosensors for Rab Family GTPases

Nanako Ishido, Hotaka Kobayashi, Yasushi Sako, Takao Arai, Mitsunori Fukuda and Takeshi Nakamura
Tokyo University of Science; Tohoku University; RIKEN
Japan

1. Introduction

Genetically-encoded Förster resonance energy transfer (FRET) biosensors enable us to visualize a variety of signaling events, such as protein phosphorylation and G protein activation in living cells (Miyawaki, 2003). Using FRET-based biosensors we can obtain spatiotemporal information on the changes in activity of signaling molecules in living cells. From this viewpoint, FRET imaging of signaling molecules that regulate membrane traffic is one of the most suitable applications of this technique. The Rab family GTPases constitute the largest branch of the Ras GTPase superfamily. Rab GTPases use the guanine nucleotide-dependent switch mechanism common to the Ras superfamily to regulate each of the four major steps in membrane trafficking: vesicle budding, vesicle delivery, vesicle tethering, and fusion of the vesicle membrane with that of the target compartment (Zerial and McBride, 2001; Grosshans et al., 2006; Stenmark, 2009). Recently, we developed a FRET sensor for Rab5, and demonstrated that live-cell imaging with FRET sensors enables us to pinpoint the activation and inactivation of Rab5, and thereby to understand its relationship with other events linked to vesicle transport (Kitano et al., 2008).

In the first half of this chapter, we describe step-by-step strategies to develop unimolecular-type FRET biosensors for Rab family GTPases. We use the development of a Rab35 sensor as an example. Although improvements to FRET sensors are still made on a trial-and-error basis, we provide practical tips for their optimization. In the second half of this chapter, we introduce FRET imaging with total internal reflection fluorescence (TIRF) microscopy. TIRF microscopy is particularly well suited to visualize the dynamics of molecules and events near the plasma membrane (Mattheyses et al., 2010). We have used FRET imaging with TIRF microscopy to show that the activity of TC10, a Rho family GTPase, at tethered vesicles drops immediately before vesicle fusion in HeLa cells stimulated with epidermal growth factor (EGF) (Kawase et al., 2006). We describe how to set up and use TIRF-FRET to visualize local changes in GTPase activity on vesicles during membrane fusion.

2. Unimolecular FRET sensors

2.1 Overview of FRET biosensors

FRET is a process by which a fluorophore (donor) in an excited state transfers its energy to a neighboring fluorophore (acceptor) non-radiatively (Tsien and Miyawaki, 1998; Pollok and

Heim, 1999). Although an understanding of the physical principles underlying FRET is not necessarily required for biological experiments, researchers who try to develop and/or use FRET sensors must note that FRET depends on a proper spectral overlap between the donor and the acceptor, the distance between both fluorophores, and their relative orientation. The physical principles underlying FRET have been extensively reviewed elsewhere (Periasamy and Day, 1999; Jares-Erijman and Jovin, 2003).

2.2 Advantages of unimolecular FRET sensors

In general, green fluorescent protein (GFP)-based FRET sensors are classified into two types: bimolecular and unimolecular sensors (Miyawaki, 2003; Kurokawa et al., 2004). For bimolecular sensors, donor (CFP) and acceptor (YFP) are fused to protein A (e.g., the sensor domain) and protein B (e.g., the detector domain), respectively (Fig. 1a). In this case, protein

(a) Bimolecular sensor, in which YFP and CFP are fused to protein A and protein B, respectively. Upon stimulation, the association of proteins A and B brings YFP in close proximity to CFP, and FRET occurs. (b) Unimolecular sensor, in which protein A and protein B are 'sandwiched' between YFP and CFP.

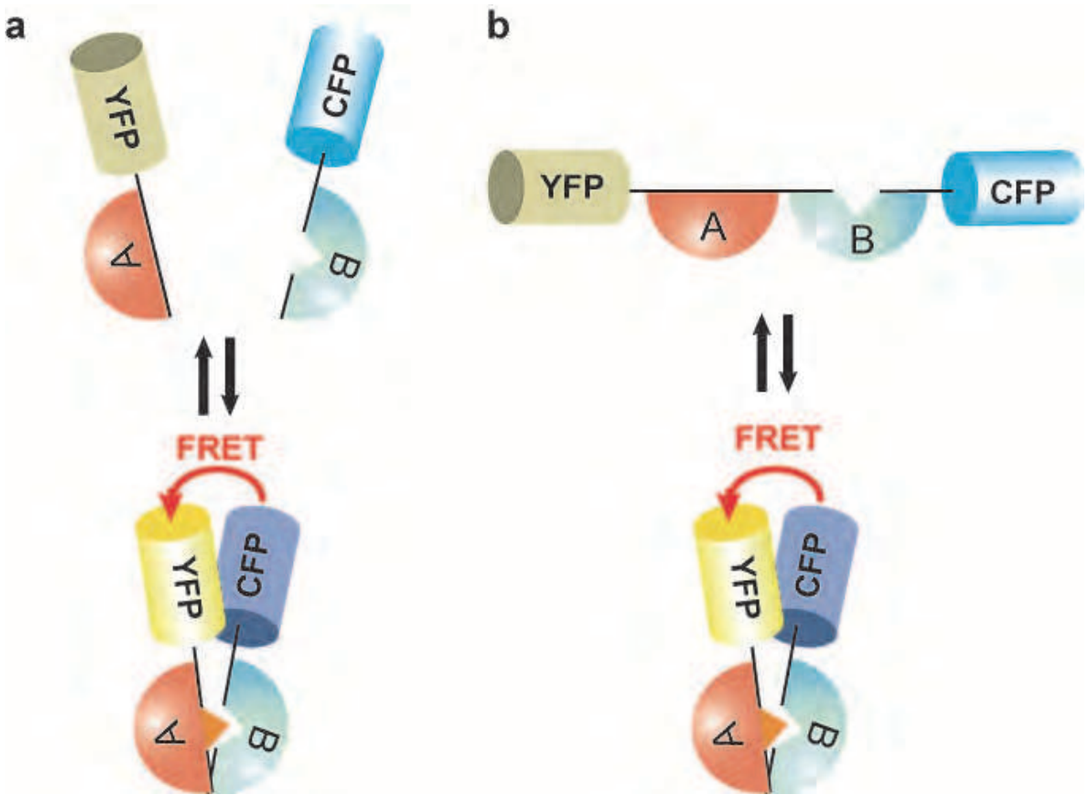

Fig. 1. Two types of FRET biosensors

A changes its conformation following stimulation. Then, protein A binds to protein B and FRET occurs. The change in distance between the fluorophores is critically important for bimolecular sensors (Fig. 1a). In contrast, for unimolecular sensors, all four modules are combined into a single chain (Fig. 1b). Also for unimolecular sensors, protein A changes its conformation following stimulation. Then, protein A binds to protein B and FRET occurs.

However, the change in distance between both fluorophores is not so large, as shown in Fig. 1b. Thus, developers of unimolecular sensors have to consider how to induce a large change in relative orientation between the fluorophores. At present, it is almost impossible to design retionally an optimal structure for a particular unimolecular sensor, and therefore its design is still labor-intensive (described in detail below).

Nevertheless, in our opinion, if good sensors are available, it is preferable to use a unimolecular sensor. This is because with a unimolecular sensor protein A and protein B are placed in close proximity, and thus, protein B can easily find protein A. This will increase the percentage of real FRET signals *versus* undesired signals arising from donor emission bleedthrough and direct acceptor excitation (Hailey et al., 2002; Kurokawa et al., 2004). Furthermore, perturbation of endogenous signaling is reduced when using a unimolecular sensor instead of a bimolecular sensor (Miyawaki, 2003). An additional drawback of bimolecular sensors is that it is difficult to conrol their expression levels, because the ideal molecular ratio of YFP-protein A and CFP-protein B is 1:1 for quantitative FRET imaging.

It should be noted that, from a general point of view, the suitable applications for bimolecular and unimolecular sensors are different. Thus, in practice, the type of sensors is chosen based on the aim of the experiment. In the case of monitoring an interaction between protein A and protein B, it is natural to select a bimolecular sensor. Correction of FRET signals obtained with a bimolecular sensor is elaborate but attainable (Kraynov et al., 2000; Sekar and Periasamy, 2003). Unimolecular sensors are preferable for visualizing changes in the activity of a protein, pH, Ca^{2+} concentration, *etc.*.

3. How to make FRET biosensors for Rab family GTPases

3.1 Raichu sensors

Unimolecular FRET sensors, which can visualize the 'on' and 'off' states of Ras GTPase superfamily proteins, were first developed in Matsuda's laboratory and are collectively designated "Ras and interacting protein chimaeric unit (Raichu)" sensors (Mochizuki et al., 2001). Similar FRET sensors for Ras GTPase superfamily proteins have been reported by other groups (Pertz et al., 2006).

Raichu sensors comprise four modules: a donor (CFP), an acceptor (YFP), a GTPase and the GTPase-binding domain of its binding partner. In the Raichu sensors for Ras family GTPases, YFP, the GTPase, the GTPase-binding domain, and CFP are sequentially connected from the N-terminus by spacers (Mochizuki et al., 2001). In the inactive GDP-bound form of the GTPase, CFP and YFP in the sensor are located at a distance from each other, mostly resulting in emission from CFP. Upon stimulation, GDP on the GTPase is exchanged for GTP, which induces an interaction between the GTP-bound GTPase and the GTPase-binding domain. This intramolecular binding brings CFP close to YFP, thereby permitting energy transfer from CFP to YFP. FRET is simultaneously manifested by a quenching of CFP fluorescence and an increase in YFP fluorescence; therefore, the YFP/CFP ratio of Raichu sensors is conveniently used as a representation of FRET efficiency. Previous experiments have shown that the YFP/CFP ratio of a Raichu sensor correlates with the GTP/GDP ratio (Mochizuki et al., 2001; Yoshizaki et al., 2003). Raichu sensors for Ras family GTPases (Ras, Rap1, Ral, R-Ras) (Mochizuki et al., 2001; Takaya et al., 2004; Takaya et al., 2007), Rho family GTPases (RhoA, Rac1, Cdc42, TC10)(Itoh et al., 2002; Yoshizaki et al., 2003), and Rab family GTPase (Rab5) (Kitano et al., 2008) have been published to date.

3.2 FRET imaging using Raichu-Rab5

Rab5 is a key regulator of a broad range of early endocytic pathway components (Zerial and McBride, 2001) including apoptotic cell engulfment (Nakaya et al., 2006). However, the precise spatio-temporal dynamics of Rab5 activity during endocytosis remain unknown. To make Rab5 activity visible in living cells, we developed a FRET biosensor for Rab5, Raichu-Rab5 (Fig. 2a). The difference between Raichu sensors for Ras and Rho GTPases and Raichu-Rab5 is the order of the four modules that constitute the FRET sensors. In the case of Raichu-Rab5, we placed Rab5 at the C-terminus, because the *in vivo* lipid modification of Rab5 requires access of Rab5-bound Rab escort protein (REP) to the lipid modification site of Rab5 located at the C-terminus of the FRET sensor. We confirmed that Raichu-Rab5 colocalized with red fluorescent protein (RFP)-Rab5 and bound to Rab guanine dissociation inhibitor (a) Schematic representation of Raichu-Rab5 bound to GDP or GTP. RBD indicates the N-terminal Rab5-binding domain of early endosome antigen 1 (EEA1). (b) $\alpha_v\beta_3$ integrin-expressing Swiss3T3 cells were transfected with pRaichu-Rab5/PM and co-cultured with apoptotic thymocytes in the presence of MFG-E8. Thereafter, images were obtained every 1 min. The top panels show PC and FRET/CFP ratio images at the indicated time-points (min). In the intensity-modulated display mode shown here, eight colors from red to blue are used to represent the FRET/CFP ratio, with the intensity of each color indicating the mean intensity of FRET and CFP. The upper and lower limits of the ratio range are shown at the bottom. Time sequences in the bottom panels show the PC, FRET/CFP ratio, and CFP images of the engulfed sites marked by white squares in the top panels. Scale bar: 20 μm. Figure reproduced with permission from Nature Publishing Group (Kitano et al., 2008).
(RabGDI). The dynamic range, *i.e.*, the percentage increase in the YFP/CFP ratio, of Raichu-Rab5 is 96%; thus, Raichu-Rab5 has the widest dynamic range among the Raichu biosensors that have been reported thus far.

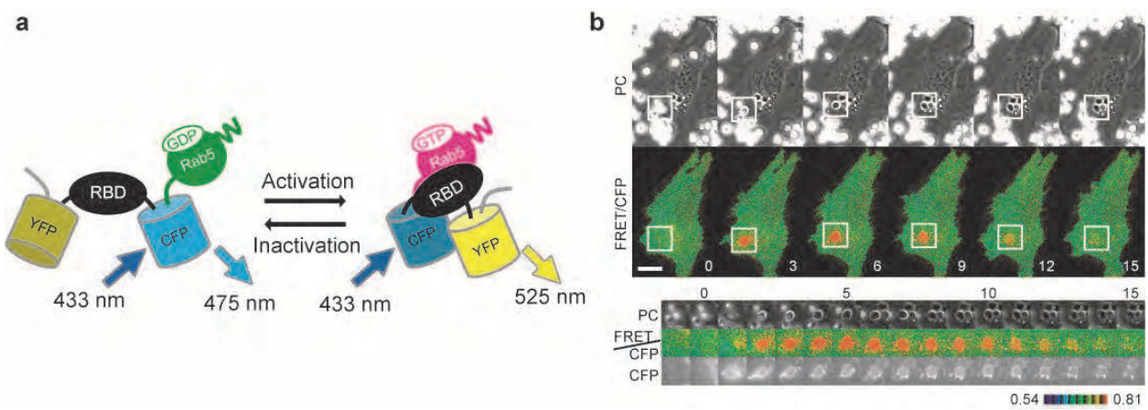

Fig. 2. FRET imaging using Raichu-Rab5

Using Raichu-Rab5 fused to the C-terminus of K-Ras protein (Raichu-Rab5/PM), we visualized Rab5 activation during milk fat globule epidermal growth factor 8 (MFG-E8)-mediated engulfment of apoptotic cells by Swiss3T3 cells stably-expressing integrin $\alpha_v\beta_3$ (Fig. 2b). The progress of phagocytosis was monitored by phase-contrast (PC) images, in which the completion of engulfment was recognizable by the transition of the engulfed apoptotic cells from phase-bright to phase-dark (Diakonova et al., 2002). We set the zero time-point to be the frame immediately before the initiation of the phase shift, which lasted

approximately 3 minutes on average. Rab5 activation started during this period of phase shift and reached a peak within an average of 4 minutes. Very similar results were obtained in the macrophage cell line, BAM3.
Visualization of the activation and inactivation of Rab5 on phagosomes has enabled us to understand its relationship with other events during phagocytosis. Engulfment of apoptotic cells and accumulation of actin filaments around nascent phagosomes preceded Rab5 activation, which occurred in parallel with actin disassembly. Microtubules were required for Rab5 activation on phagosomes, suggesting that the actin coat around the phagosome behaves as a physical barrier to microtubule extension. This view was supported by the finding that Gepex-5, which was located at microtubule tips through binding to EB1, was responsible for Rab5 activation on phagosomes.

3.3 Development of Raichu-Rab35

3.3.1 Overview of Rab35

Rab35, whose transcripts are apparently ubiquitously expressed (Zhu et al., 1994), bears the closest homology with yeast Ypt1p and mammalian Rab1a and Rab1b, which function in endoplasmic reticulum-Golgi transport. However, Rab35 does not show an endoplasmic reticulum-Golgi localization. Endogenous Rab35 in HeLa cells is found mainly at the plasma membrane and in the cytosol, with labeling of intracellular endosomal structures identifiable at the ultrastructural level (Kouranti et al., 2006).
Recent analyses in different systems have revealed an amazingly diverse array of Rab35 functions (Table 1). Acting in the context of endosomal trafficking and recycling, Rab35 has been shown to regulate cytokinesis of *Drosophila* S2 cells and HeLa cells (Kouranti et al., 2006), oocyte receptor recycling in *Caenorhabditis elegans* (Sato et al., 2008), and Ca^{2+} activated potassium channel recycling (Gao et. al., 2010). In immune cells, Rab35 is implicated in T-cell receptor recycling, immunological synapse formation (Patino-Lopez et al., 2008), and major histocompatibility complex (MHC) class II molecule recycling (Walseng et al., 2008). Connecdenn/DENND1A, a guanine nucleotide exchange factor (GEF) for Rab35, plays a role in synaptic vesicle endocytosis/recycling (Allaire et al., 2006) and cargo-specific exit from early endosomes (Allaire et al., 2010).
Another facet of Rab35's function is the promotion of cellular protrusions. In baby hamster kidney (BHK) cells, overexpression of wild type or a constitutively active mutant of Rab35 induced the formation of long cell extensions, while the GDP-locked mutant of Rab35 constitutively active mutant of Rab35 also induced neurite outgrowth in N1E-115 and PC12 cells (Chevallier et al., 2009; Kanno et al., 2009). Expression of wild-type Rab35 in S2 cells induced filopodia-like cellular extensions, a process that was blocked with an inhibitor of actin polymerization (Zhang et al., 2009). The authors claimed that Rab35 controls actin bundling. Very recently, Rab35 has been reported to regulate exosome secretion in oligodendrocytes. These authors suggested that Rab35 might function in docking or tethering (Hsu et al., 2010)
Key questions in the understanding of the wide range of Rab35 functions are (i) what exactly is the role of Rab35 in recycling endosome-cell surface transport, and (ii) how does its function intersect with that of Rab11? The membrane localization patterns of Rab35 and Rab11 show a large degree of overlap. It also appears that Rab35 and Rab11's gross membrane traffic functions overlap substantially, and manipulation of their activities affects common recycling cargos such as the transferrin receptor (Chua et al., 2010). One scenario is

Function	Animal/Cell	Reference
endosomal trafficking and recycling		
cytokinesis	*Drosophila* S2 cells, HeLa cells	Kouranti et al. (2006)
transferrin recycling	HeLa cells	Kouranti et al. (2006)
synaptic vesicle recycling	hippocampal neurons	Allaire et al. (2006, 2010)
york receptor recycling	*C. elegans*	Sato et al. (2008)
T cell receptor recycling	Jurkat cells	Patino-Lopez et al. (2008)
MHC-II recycling	HeLa cells expressing MHC-II	Walseng et al. (2008)
immunological synapse formation	Jurkat and Raji cells	Yuseff et al. (2009)
Ca^{2+}-activated K channel recycling	HEK and HMEC-1 cells	Gao et al. (2010)
peripheral protrusion formation	BHK cells	Chavallier et al. (2009)
neurite outgrowth	N1E-115 and PC12 cells	Chavallier et al. (2009)
bristle formation	*Drosophila*	Zhang et al. (2009)
exosome secretion	Oli-neu cells	Hsu et al. (2010)

Table 1. The broad range of functions of Rab35

that Rab11 and Rab35 function sequentially in recycling endosomes to plasma membrane transport, similarly to the Rab11 to Rab8 pathway in AMPA receptor trafficking in dendritic spines (Brown et al., 2007). On the other hand, transport carried from recycling endosomes could require both Rab11 and Rab35 in proportions determined by the types of membrane cargo in a cell type specific, or cell physiology-dependent manner. Defining the pathways and factors involved in Rab11 and Rab35 functions in different endocytic recycling systems is clearly of immediate interest. Furthermore, we emphasized that FRET imaging is the most suitable and reliable tool to examine local activity regulation in these dynamic systems.

3.3.2 A practical guide to making FRET biosensors for Rab family GTPases

The following is an abridged procedure for developing Raichu-type FRET sensors for Rab GTPases essentially based on the protocol to make Raichu sensors for Ras and Rho GTPases (Nakamura et al., 2006; Nakamura and Matsuda, 2009; Kiyokawa et al., 2011).

Design of a candidate sensor

As described above, it is almost impossible to design rationally an optimal structure for a desired unimolecular sensor. Thus, at first, developers should identify as many proteins as possible that bind to the target Rab in a GTP-dependent manner. Empirically, we like to collect three to five binding proteins that have different affinities for the target Rab protein. The developers should also collect informations about the protein motifs required for the binding.

One way to make a sensor with a wide dynamic range is to search for a GTPase-binding domain that has a moderate affinity for the GTPase (Yoshizaki et al., 2003). One explanation for this is that the GTPase-binding domain competes with the GTPase activating proteins (GAPs) in cells (Kurokawa et al., 2004). Strong inhibition of GAPs would lead to a relatively high GTP level in the sensor, even in the unstimulated state, which may cause a narrowing of the dynamic range.

Crystallographic data for the GTPase and GTPase-binding domain can help to determine the minimum regions to incorporate into the sensor. Unfortunately, there is currently insufficient crystallographic data for the optimal design of a Raichu sensor in most cases. Therefore, trying various lengths of the GTPase and GTPase-binding domain is highly recommended. In addition, various sequential combinations of the four modules (YFP, CFP, GTPase, and GTPase-binding domain) should be tested. YFP is usually located before CFP because an excess of the acceptor (YFP) does not greatly decrease the signal-to-noise ratio, even when translation of the sensor is prematurely terminated. Eleven amino acids at the C-terminus of GFP can be truncated without affecting its fluorescence profile. In most Raichu sensors, we have removed the 11 C-terminal residues of YFP, hoping to reduce the flexibility between YFP and the subsequent module. The length and sequence of the spacers are also critical. If the FRET efficiency of a prototype sensor changes to some extent upon activation, the possibility of further improvement by changing the spacer should be considered. As spacers, we usually use one to six repeats of the sequence Gly-Gly-Ser-Gly-Gly; however, we intend to reexamine this in a future. It is considered that Gly provides flexibility, while Ser prevents aggregation of peptide chains. Misfolding of CFP occasionally occurs, and this can sometimes be rectified by modifying the spacer before the CFP.

If developers obtain a candidate sensor whose dynamic range is broad enough, the next step is further optimization. At present, the principle of this optimization step is a matter of debate. Recently, Nagai's group reported two strategies for sensor optimization (Kotera et al., 2010). They claim that the balance between the enhancement of dimerization and the maintenance of free dissociation is critical; among the *Aequorea* fluorescent protein variants they examined, those with alanine at 206 most closely matched the requirements. Kotera and collegues also claimed that developers should note the relative orientation of the fluorescent proteins. For the fluorescent proteins to dimerize, they must be bound in an antiparallel configuration. Because wildtype GFP has both N- and C-termini in close proximity, at least in the crystal (Palm et al., 1997), simple fusion of fluorescent proteins with a short linker will not result in antiparallel dimerization. Nagai's group presumed that the effectiveness of circular permutation (cp) mutants in several FRET sensors, such as yellow cameleon 3.6 (Nagai et al., 2004), might come from the ease of dimerization of fluorescent proteins in an antiparallel configuration.

The ideal location for a sensor in a cell has also been a matter of debate. The most persuasive idea is that the sensor should be colocalized with the endogenous protein; for this purpose, the GTPase's own CAAX-box should be added to the C-terminus of the sensor. As described for Raichu-Rab5, it is necessary to place Rab protein at the C-terminus because *in vivo* lipid modification of Rab requires access by Rab-bound REP to the lipid modification site of the Rab protein located at the C-terminus of the FRET sensor. Alternatively, addition of the CAAX-box of K-Ras4B to the C-terminus enables the sensor to be located at the plasma membrane; this approach mostly yields a high signal-to-noise ratio, especially when only a limited fraction of the GTPase is activated upon stimulation. If a fraction of the target Rab protein resides in the plasma membrane and is expected to change its activity there upon stimulation, this type of FRET sensor might be useful as shown for Raichu-Rab5.

Characterization of candidate sensors

We usually transfect candidate sensors into the FreeStyle 293-F cell line (Invitrogen), which is a variant of the 293 cell line adapted for suspension growth. Following a 2-day incubation, the cell culture is poured into 3-ml cuvettes and the cuvettes are placed in a

spectrophotometer (for example, a JASCO FP-6200). Next, we illuminate the cell culture with an excitation wavelength of 433 nm, and obtain a fluorescence spectrum from 450 nm to 550 nm. The background is subtracted using the spectrum of the mock-transfected cell culture.

If developers do not use 293-F cells, 293T cells plated on 100-mm collagen-coated dishes should be transfected with candidate sensors, and cell lysates prepared according to a standard procedure should be used for fluorescence spectrometry (Nakamura and Matsuda, 2009).

For characterizing a candidate sensor, we introduce a constitutively active or inactive mutation into the GTPase in the sensor for comparison with the same sensor containing the wild-type GTPase. Alternatively, we co-transfect the candidate sensor with a GEF or GAP for the GTPase, and compare the spectrum with those of samples transfected with the sensor alone. Under our criteria, Raichu-type sensors are considered suitable for FRET imaging when the dynamic range exceeds 30%.

Practically, further evaluation of a sensor is recommended before widespead use. We recommend that developers check the following: (i) whether the sensor shows a linear correlation between its GTP loading and FRET efficiency upon cotransfection with various quantities of GEFs or GAPs and (ii) whether the sensor and its endogenous counterpart show comparable responses to physiological stimulations when examined by biochemical methods.

3.3.3 Example: development of Raichu-Rab35

To make Rab35 activity visible in living cells, we developed FRET sensors, designated Raichu-Rab35s. We used centaurinβ2 (Kanno et al., 2010) and Rab35BP2 (Kobayashi et al., submitted) for the Rab35 effector proteins. We constructed sensors based on either the basic structure of Raichu-Rab5 containing m1Venus and m1SECFP as fluorescent proteins (Kitano et al., 2008) or the newly-developed design in Matsuda's laboratory (Komatsu et al., unpublished) containing YPet (Nguyen and Daugherty, 2005) and SECFP.

In the initial tests, Raichu-A011 showed the broadest dynamic range over 30% (Table 2). However, the FRET/CFP ratio of the sensor containing wild-type Rab35 is almost similar to that of the sensor containing Rab35-Q67L, suggesting that Raichu-A011 might be almost insensitive to Rab35GEF. The dynamic range of Raichu-A018 was relatively high (24.3%) and the cellular localization of Raichu-A018 resembled that of EGFP-Rab35. As shown in the left panel of Fig. 3, Raichu-A018 is expected to respond to both GEFs and GAPs.

Although the dynamic range of Raichu-A008 and Raichu-A015 was promisingly broad, the FRET/CFP ratio of the sensor containing Rab35-S22N was higher than that of the sensor containing Rab35-Q67L. Based on our experience, we tentatively excluded these two candidates because sensors with these characteristics cannot generally respond to GEFs and GAPs. At this stage, we thought that Rab35BP2 might be more suitable than centaurinβ2 as an effector protein. Thus, in the next step, we prepared candidate sensors containing Rab35BP2-RBD.

Next, we tried two approaches. First, we used the minimal Rab35-binding domain, Rab35BP2-RBDΔC2, which was identified during the course of Raichu-Rab35 development. Second, we replaced YPet with cp mutants of Venus to change the relative orientation of the fluorescent proteins. As a result, we obtained two more promising candidate sensors: Raichu-A033 and Raichu-A050. Raichu-A033 has a remarkably broad dynamic range

Sensor name	Basic design	Binding domain	Yellow FP	Dynamic range
Raichu-A008	Raichu-Rab5 type	centaurinβ2-RBD	m1Venus	-22.5%
Raichu-A011	Raichu-Rab5 type	Rab35BP2-RBD	m1Venus	33.7%
Raichu-A015	Long-linker type	centaurinβ2-RBD	YPet-M	-23.3%
Raichu-A018	Long-linker type	Rab35BP2-RBD	YPet-M	24.3%
Raichu-A030	Raichu-Rab5 type	Rab35BP2-RBD-ΔC2	m1Venus	21.6%
Raichu-A033	Long-linker type	Rab35BP2-RBD-ΔC2	YPet-M	92.7%
Raichu-A036	Long-linker type	Rab35BP2-RBD	cp195Venus	24.8%
Raichu-A039	Long-linker type	Rab35BP2-RBD	cp173Venus	16.9%
Raichu-A047	Long-linker type	Rab35BP2-RBD-ΔC2	cp195Venus	41.1%
Raichu-A050	Long-linker type	Rab35BP2-RBD-ΔC2	cp173Venus	37.0%

Table 2. Summary of candidate FRET sensors for Rab35

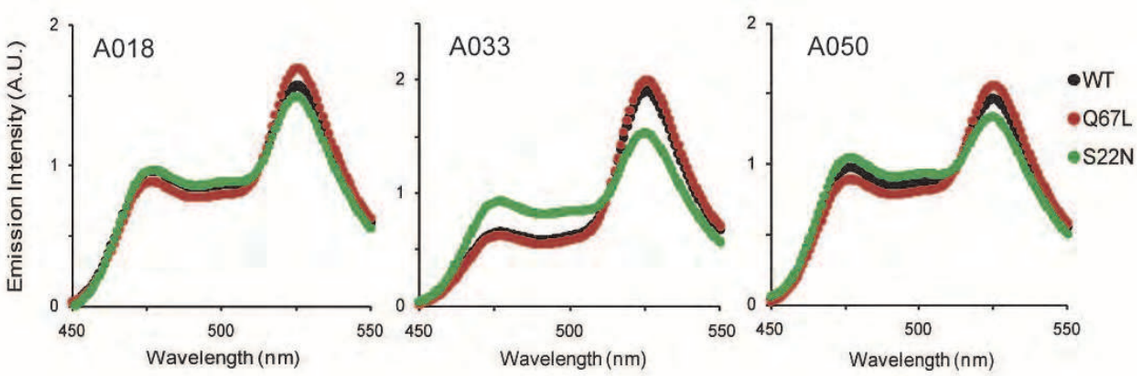

Fig. 3. Emission spectra of Raichu-Rab35s

Sensor name	Binding domain	Yellow FP	Dynamic range	Presumed property
Raichu-A018	Rab35BP2-RBD	YPet-M	24.3%	highly sensitive to GEF
Raichu-A033	Rab35BP2-RBD-ΔC2	YPet-M	92.7%	highly sensitive to GAP
Raichu-A050	Rab35BP2-RBD-ΔC2	cp195Venus	37.0%	sensitive to GEF and GAP

Table 3. Summary of FRET sensors for Rab35

(92.7%), which is comparable to that of Raichu-Rab5 described above. However, as shown in Fig. 3, the FRET/CFP ratio of this sensor containing wild-type Rab35 is very similar to that of the sensor containing Rab35-Q67L, suggesting that Raichu-A033 might be somewhat insensitive to Rab35GEF (Fig. 3, middle). For the other candidate, Raichu-A050, the dynamic range is sufficiently high (37.0%) and it is expected to respond to both GEFs and GAPs (Fig. 3, right), although its cellular localization is somewhat different from that of EGFP-Rab35. Table 3 shows a summary of the features of our newly developed Rab35 sensors. We believe that different Rab35 sensors may suit different situations.
293-F cells expressing Raichu-A018, A033, and A050 were excited at 433 nm and a fluorescent spectrum from 450 nm to 550 nm was obtained. WT, Q67L, and S22N denote wild-type, constitutively active mutant, and GDP-locked mutant, respectively.

4. How to use the TIRF-FRET system

4.1 General considerations

TIRF microscopy provides a means to excite fluorophores selectively near the adherent cell surface while minimizing fluorescence from intracellular regions. TIRF primarily illuminates only fluorophores very near (*i.e.,* within 100 nm of) the cover slip–sample interface. Background fluorescence is minimized because excitation of fluorophores further away from the cover slip is drastically reduced. For this reason, TIRF has been employed to address numerous questions regarding the dynamics of the cytoskeleton or intracellular signaling near the plasma membrane, endocytosis, exocytosis, and cell–substrate contacts (Mattheyses et al., 2010).
Several studies using FRET imaging under TIRF microscopy have been reported since 2003. However, all of these studies have used bimolecular FRET sensors to investigate protein–protein interaction (Bal et al., 2008; Lam et al., 2010) or cAMP signaling (Dyachok et al., 2006). In 2006, we reported FRET imaging using the unimolecular sensor Raichu–TC10 under TIRF microscopy during EGF-induced exocytosis (Kawase et al., 2006). To our knowledge, this was the first report of TIRF imaging using a unimolecular FRET sensor.

4.2 Visualization of GTP hydrolysis of TC10 during exocytosis using TIRF-FRET system

TC10, a Rho-family GTPase, plays a significant role in the exocytosis of GLUT4 (Chiang et al., 2001; Saltiel and Pessin, 2002) and other proteins (Cuadra et al., 2004; Cheng et al., 2005). Furthermore, TC10 is mainly localized to vesicular structures (Michaelson et al., 2001), which makes it suitable for monitoring activity changes on vesicles. In Kawase et al. (2006), we reported visualization of GTP hydrolysis of TC10 immediately before vesicle fusion, using a combination of a newly developed unimolecular FRET sensor, Raichu-TC10, and TIRF microscopy (Fig. 4). We postulated that hydrolysis of GTP-TC10 triggers vesicle fusion. In support of this model, a GTPase-deficient TC10 mutant potently inhibited EGF-induced vesicular fusion in HeLa cells and depolarization-induced secretion of neuropeptide Y in PC12 cells. Our study also indicated that GTP-TC10 is indispensable for loading its binding partners onto vesicles, and for the delivery of vesicles to target membranes. Thus, TC10 could play roles in three separate steps of exocytosis: loading of the cargo, tethering to the plasma membrane, and triggering vesicle fusion. Of note, both GTP-loading and GTP

hydrolysis of TC10 play important roles and occur simultaneously in different subcellular compartments. Therefore, functional imaging of GTPases using FRET-based sensors is very powerful for the analysis of parallel events within the same cell.

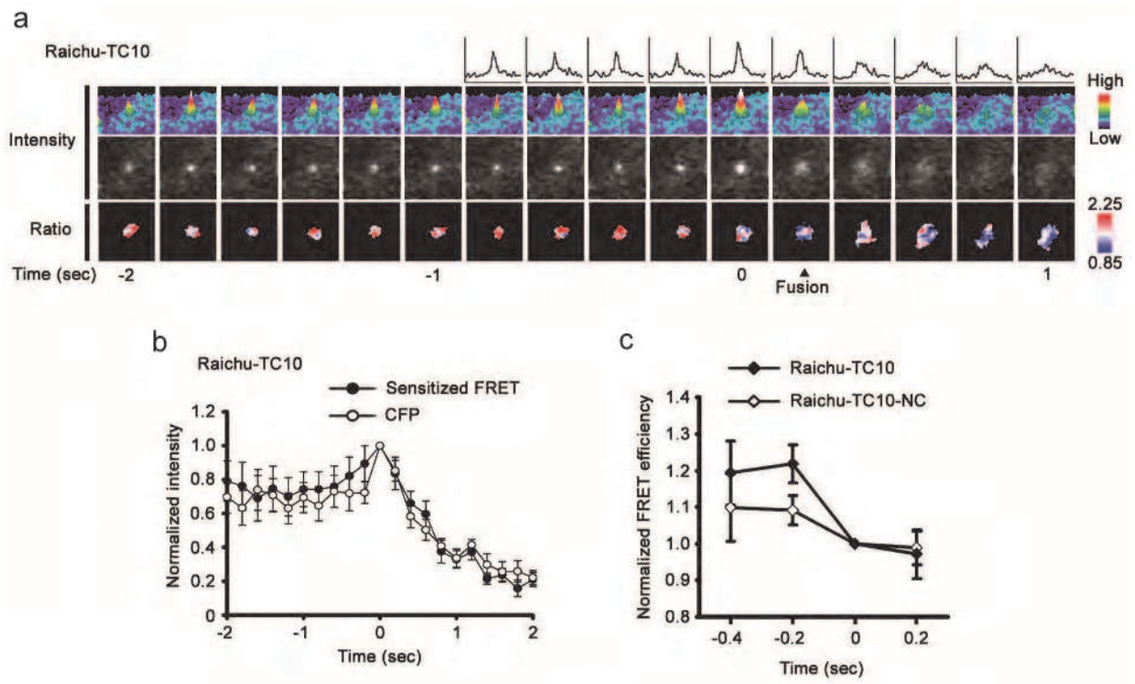

Fig. 4. GTP hydrolysis of TC10 immediately before fusion

(a) Sensitized FRET intensity and ratio images of Raichu-TC10 in fusing vesicles obtained by TIRF microscopy. The first and second rows show plots of the sensitized FRET intensity scanned across the center of the fusing vesicles, and pseudocolored 3D-plots of the sensitized FRET intensity, respectively. (b) Time-course of normalized sensitized FRET and CFP intensities of vesicles containing Raichu-TC10. (c) Time-dependent changes in the normalized FRET efficiency of Raichu-TC10- or Raichu-TC10-NC- (a negative control)-expressing vesicles. The bars in (b,c) are SEM (Raichu-TC10, n = 8; Raichu-TC10-NC, n = 11). Reprinted from Developmental Cell, Vol. 11, Kawase, Nakamura, Takaya, Aoki, Namikawa, Kiyama, Inagaki, Takemoto, Saltiel, and Matsuda, "GTP hydrolysis by the Rho family GTPase TC10 promotes exocytic vesicle fusion", 411–421, ©2006, with permission from Elsevier.

4.3 Setting up of a TIRF-FRET system

Although many researchers use 'home-made' TIRF set-ups, commercial TIRF systems are available from major microscopy companies (Olympus, Nikon, Zeiss, and Leica). These systems have the same fundamental ability to deliver a through-the-objective TIRF illumination and can be used to obtain TIRF-FRET images. Prism-based TIRF has several benefits, including lower cost and a clearer evanescent field; however most cell biologists use a through-the-objective TIRF system, because it is more user-friendly, requiring minimal maintenance and alignment.

One important requirement in through-the-objective TIRF is the use of high numerical aperture (NA) objectives. The NA of an objective describes its light-gathering power and also describes the maximum angle at which the excitation light can emerge from the objective. Therefore, the NA of the objective must be greater than the refractive index of the sample, preferable by a substantial margin. There are several commercial TIRF objectives with an NA greater than 1.4. The most common TIRF objectives are 1.45 NA and 1.49 NA, and both are available in 60× and 100× options.

There is a wide range of charge-coupled device (CCD) cameras from conventional CCDs to electron-multiplying (EM) CCDs. For TIRF-FRET imaging in the field of membrane traffic, EMCCDs are strongly recommended because rapid imaging in very low light situations is required. In addition, an image splitter, which allows simultaneous acquisition of emission from two spectrally distinct fluorophores, offers great benefit in obtaining FRET from moving vesicles. However, users should note that the image splitter can cause a problem, known as a misregistration, when generating FRET images.

In TIRF-FRET imaging using Raichu-TC10, we used an Olympus IX70 inverted microscope equipped with a 442-nm HeCd laser (Omnichrome), a TIRF illuminator (Olympus), and an Olympus 100x objective (NA 1.45). The CFP and sensitized images were obtained simultaneously using an image splitter (Dual-View; Optical Insights) and an EMCCD camera (iXon DV887; Andor) as shown in Fig. 5.

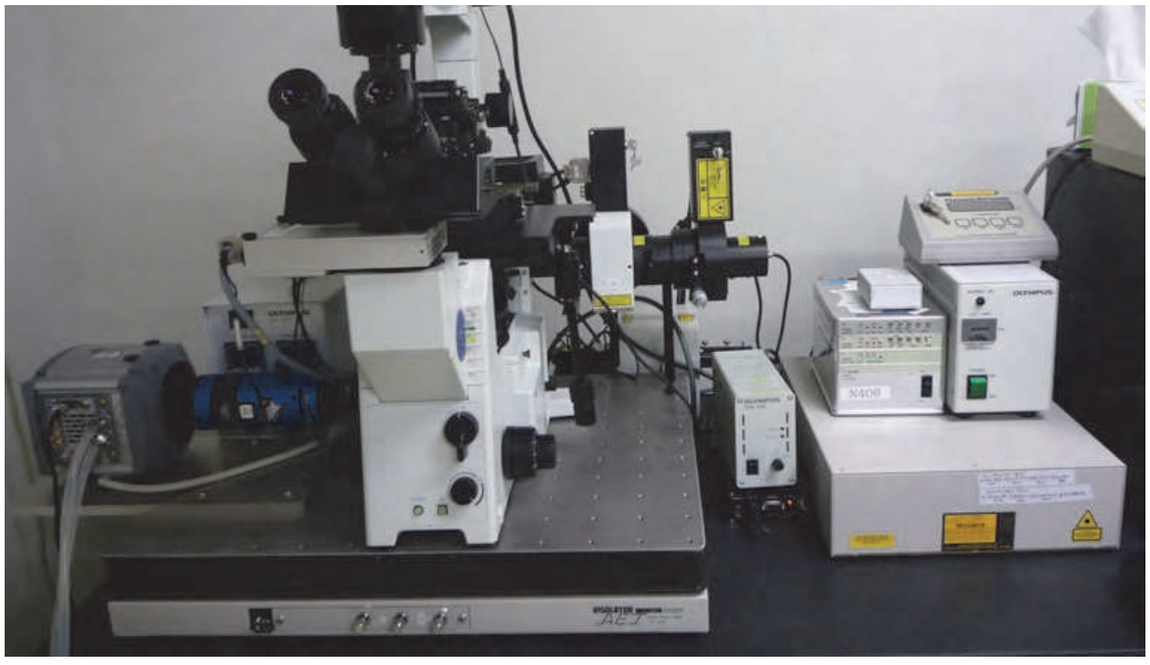

Fig. 5. One example of a TIRF-FRET system

Commercially available TIRF microscopes use one-sided laser illumination. However, in this method, the interference patterns of lasers sometimes reduce the quality of the image. Furthermore, the concave shape of cells and anisotropic cellular structures might reduce the image quality. These issues can be overcome by illumination from several directions using multiple beams or a circular laser beam (Sako, 2006).

4.4 Image acquisition

TIRF-FRET imaging is conducted similarly to conventional FRET imaging (Nakamura and Matsuda, 2009). In the case of Raichu-TC10 imaging (Fig. 4), plasmids encoding Raichu-TC10 were transfected into HeLa cells plated on glass-bottomed dishes. After 24 h, the cells were starved for 3 h and then stimulated with 50 ng/ml of EGF. The FRET efficiency (sensitized FRET/CFP ratio) in the subcellular compartments was determined as follows. For vesicles and perinuclear compartments, regions showing higher CFP intensity than an appropriate threshold level were selected, and their sensitized FRET and CFP intensities were obtained. For the plasma membrane, three appropriate regions were selected manually and the averages of their sensitized FRET and CFP intensities were obtained. Images were obtained in a stream (free-run) mode using MetaMorph software (Universal Imaging); stacked images containing 500 planes were continually acquired with a 200-ms exposure.

The most common problem with TIRF microscopy is contamination of the image with propagating light (Matteyses et al., 2010). The most likely reason for this is an improperly aligned excitation source. This will be readily recognized as a field that is half in and half out of TIRF, or the complete inability to obtain TIRF. The excitation laser beam must be focused on the back focal plane of the objective. If this is not the case, light will emerge from the objective at multiple angles. It is important to follow the manufacturer's instructions to check and correct the focus onto the back focal plane.

4.5 Image analysis

Images obtained during vesicular fusion (Kawase et al., 2006) were analyzed using MetaMorph software according to Tsuboi et al. (2004), with some modifications. Image analysis is described in detail in Fig. 6.

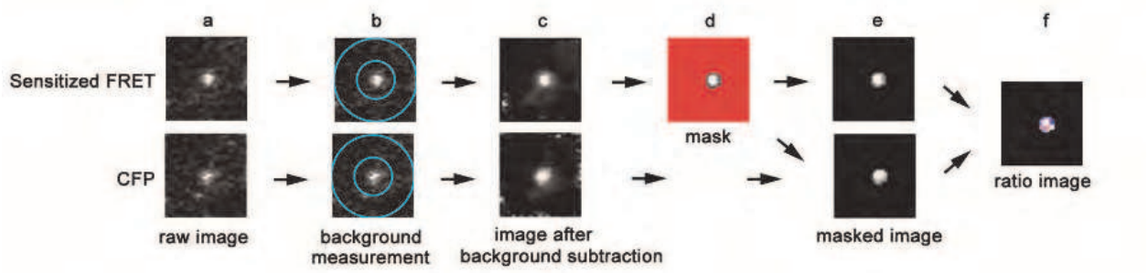

Fig. 6. Method of image processing to obtain ratio images of FRET sensors in vesicles obtained by TIRF microscopy

Single exocytotic events were selected manually, and vesicular fusion was distinguished from vesicle retreat as described previously (Fix et al., 2004). The fusing vesicle was centerd in the image (Fig. 6a). The local background was determined as the average fluorescence of the region between two concentric rings with diameters of 2 μm (inner) and 5 μm (outer) (Fig. 6b). This background was subtracted from a raw image (Fig. 6c). Next, in the sensitized FRET image, the threshold value appropriate for extracting vesicles was determined manually (Fig. 6d). This threshold mask was applied to both the sensitized FRET and the CFP images (Fig. 6e). Finally, a ratio image was obtained by dividing the sensitized FRET image by the CFP image (Fig. 6f). Reprinted from Developmental Cell, Vol. 11, Kawase, Nakamura, Takaya, Aoki, Namikawa, Kiyama, Inagaki, Takemoto, Saltiel, and Matsuda,

"GTP hydrolysis by the Rho family GTPase TC10 promotes exocytic vesicle fusion", 411-421, ©2006, with permission from Elsevier.

5. Conclusion

FRET-based biosensors for Rab family GTPases have become very powerful tools for the analysis of molecular mechanisms regulating a broad range of membrane trafficking events. In this chapter, we have provided a practical guide to making FRET sensors for Rab GTPases. In the near future, we expect further improvements in sensor design and optimization, because FRET techniques are becoming essential tools in cell biology.

6. Acknowledgments

We thank Sayaka Yoshiki and Hiroko Koizumi for technical help and their input, and members of the Matsuda laboratory for fruitful discussions. This work was supported by grants from the Ministry of Education, Culture, Sports, Science, and Technology of Japan, the Uehara Memorial Foundation, the Research Foundation for Opto-Science and Technology, and the Naito Foundation.

7. References

Allaire, P. D.; Ritter, B.; Thomas, S.; Burman, J. L.; Denisov, A. Y.; Legendre-Guillemin, V.; Harper, S. Q. ; Davidson, B. L.; Gehring, K. & McPherson, P. S. (2006). Connecdenn, a novel DENN domain-containing protein of neuronal clathrin-coated vesicles functioning in synaptic vesicle endocytosis. *Journal of Neuroscience,* 26, 13202-13212.

Allaire, P. D.; Marat, A. L.; Dall'Armi, C.; Di, P. G.; McPherson, P. S. & Ritter, B. (2010). The Connecdenn DENN domain: a GEF for Rab35 mediating cargo-specific exit from early endosomes. *Molecular Cell,* 37, 370-382.

Bal, M.; Zaika, O.; Martin, P. & Shapiro, M. S. (2008). Calmodulin binding to M-type K+ channels assayed by TIRF/FRET in living cells. *Journal of Physiology* 586, 2307-2320.

Brown, T. C.; Correia, S. S.; Petrok, C. N. & Esteban, J. A. (2007). Functional compartmentalization of endosomal trafficking for the synaptic delivery of AMPA receptors during long-term potentiation. *Jounal of Neuroscience,* 27, 13311-13315.

Cheng, J.; Wang, H. & Guggino, W. B. (2005). Regulation of Cystic Fibrosis Transmembrane Regulator Trafficking and Protein Expression by a Rho Family Small GTPase TC10. *Journal of Biological Chemistry,* 280, 3731-3739.

Chevallier, J.; Koop, C.; Srivastava, A.; Petrie, R. J., Lamarche-Vane, N. & Presley, J. F. (2009). Rab35 regulates neurite outgrowth and cell shape. *FEBS Letters,* 583, 1096-1101.

Chiang, S. H.; Baumann, C. A.; Kanzaki, M.; Thurmond, D. C.; Watson, R. T.; Neudauer, C. L.; Macara, I. G.; Pessin, J. E. & Saltiel, A. R. (2001). Insulin-stimulated GLUT4 translocation requires the CAP-dependent activation of TC10. *Nature,* 410, 944-948.

Chua, C. E. L., Lim, Y. S. & Tang, B. L. (2010). Rab35 - a vesiclular traffic-regulating small GTPase with actin modulating roles. *FEBS Letters,* 584, 1-6.

Cuadra, A. E.; Kuo, S. H.; Kawasaki, Y.; Bredt, D. S. & Chetkovich, D. M. (2004). AMPA Receptor Synaptic Targeting Regulated by Stargazin Interactions with the Golgi-Resident PDZ Protein nPIST. *Journal of Neuroscience,* 24, 7491-7502.

Diakonova, M.; Bokoch, G. & Swanson, J. A. (2002). Dynamics of cytoskeletal proteins during Fcgamma receptor-mediated phagocytosis in macrophages. *Molelular Biology of the Cell,* 13, 402-411.

Dyachok, O.; Isakov, Y.; Sagetorp, J. & Tengholm, A. (2006). Oscillations of cyclic AMP in hormone-stimulated insulin-secreting beta-cells. *Nature,* 439, 349-352.

Fix, M.; Melia, T. J.; Jaiswal, J. K.; Rappoport, J. Z.; You, D.; Sollner, T. H., Rothman, J. E. & Simon, S. M. (2004). Imaging single membrane fusion events mediated by SNARE proteins. *Proceedings of the National Academy of Science of the United Staes of America,* 101, 7311-7316.

Gao, Y., Balut, C. M., Bailey, M. A., Patino-Lopez, G., Shaw, S. & Devor, D. C. Recycling of theCa^{2+}-activated K^+ channel, KCa2.3, is dependent upon RME-1, Rab35/EPI64C, and an N-terminal domain. *Journal of Biological Chemistry,* 285, 17938-17953.

Grosshans, B. L.; Ortiz, D. & Novick, P. (2006). Rabs and their effectors: achieving specificity in membrane traffic. *Proceedings of the National Academy of Science of the United Staes of America,* 103, 11821-11827.

Hailey, D. W.; Davis, T. N. & Muller, E. G. (2002). Fluorescence resonance energy transfer using color variants of green fluorescent protein. *Methods in Enzymology,* 351, 34-49.

Hsu, C., Morohashi, Y., Yoshimura, S., Manrique-Hoyos, N., Jung, S., Lauterbach, M. A., Bakhti, M., Grønborg, M., Möbius, W., Rhee, J., Barr, F. A. & Simons, M. (2010) Regulation of exosome secretion by Rab35 and its GTPase-activating proteins TBC1D10A-C. Journal of Cell Biology 189, 223-232.

Itoh, R. E.; Kurokawa, K.; Ohba, Y.; Yoshizaki, H.; Mochizuki, N. & Matsuda, M. (2002). Activation of rac and cdc42 video imaged by fluorescent resonance energy transfer-based single-molecule probes in the membrane of living cells. *Molecular and Cellular Biology,* 22, 6582-6591.

Jares-Erijman, E. A. & Jovin, T. M. (2003). FRET imaging. *Nature Biotechnoogy,* 21, 1387-1395.

Kanno, E.; Ishibashi, K.; Kobayashi, H.; Matsui, T.; Ohbayashi, N. & Fukuda, M. (2010). Comparative screening for novel Rab-binding proteins by GST pull-down assay using 60 different mammmalian Rabs. *Traffic,* 44, 491-507.

Kawase, K.; Nakamura, T.; Takaya, A.; Aoki, K.; Namikawa, K.; Kiyama, H.; Inagaki, S.; Takemoto, H.; Saltiel, A. R. & Matsuda, M. (2006). GTP hydrolysis by the Rho family GTPase TC10 promotes exocytic vesicle fusion. *Developmental Cell,* 11, 411-421.

Kitano, M.; Nakaya, M.; Nakamuta, T.; Nagata, S. & Matsuda, M. (2008). Imaging of Rab5 activity identifies essential regulators for phagosome maturation. *Nature,* 453, 241-245.

Kiyokawa, E.; Aoki, K.; Nakamura, T. & Matsuda, M. Spatiotemporal regulation of small GTPases as revealed by probes based on the principle of Förster resonance energy transfer (FRET): implications for signaling and pharmacology. *Annual Review of Pharmacology and Toxicology,* in press.

Kotera, I.; Iwasaki, T.; Imamura, H.; Noji, H. & Nagai, T. (2010). Reversible dimerization of Aequorea victoria fluorescent proteins increases the dynamic range of FRET-based indicators. *ACS Chemical Biology,* 5, 215-222.

Kouranti, I.; Sachse, M.; Arouche, N.; Goud, B. & Echard, A. (2006). Rab35 regulates an endocytic recycling pathway essential for the terminal steps of cytokinesis. *Current Biology,* 16, 1719-1725.

Kraynov, V. S.; Chamberlain, C.; Bokoch, G. M.; Schwartz, M. A.; Slabaugh, S. & Hahn, K. M. (2000). Localized Rac activation dynamics visualized in living cells. *Science,* 290, 333-337.

Kurokawa, K.; Takaya, A.; Fujioka, A.; Terai, K. & Matsuda, M. Visualizing the signal transduction pathways in living cells with GFP-based FRET probes. (2004.) *Acta Histochemica Cytochemica,* 37, 347-355.

Lam, A. D.; Ismail, S.; Wu, R.; Yizhar, O.; Passmore, D. R.; Ernst, S. A. & Stuenkel, E. L. (2010). Mapping dynamic protein interactions to insulin secretory granule behavior with TIRF-FRET. *Biophysical Journal,* 99, 1311-1320.

Mattheyses, A .L.; Simon, S. M. & Rappoport, J. Z. (2010). Imaging with total internal reflection fluorescence microscopy for the cell biologist. *Journal of Cell Science,* 123, 3621-3628.

Michaelson, D., Silletti, J., Murphy, G., D'Eustachio, P., Rush, M. & Philips, M. R. (2001). Differential localization of Rho GTPases in live cells: regulation by hypervariable regions and RhoGDI binding. *Journal of Cell Biology,* 152, 111-126.

Miyawaki, A. (2003). Visualization of the spatial and temporal dynamics of intracellular signaling. *Developmental Cell, 4,* 295-305.

Mochizuki, N.; Yamashita, S.; Kurokawa, K.; Ohba, Y.; Nagai, T.; Miyawaki, A. & Matsuda, M. (2001). Spatio-temporal images of growth-factor-induced activation of Ras and Rap1. *Nature,* 411, 1065-1068.

Nagai, T.; Yamada, S.; Tominaga, T.; Ichikawa, M. & Miyawaki, A. (2004). Expanded dynamic range of fluorescent indicators for Ca2+ by circularly permuted yellow fluorescent proteins. *Proceedings of the National Academy of Science of the United Staes of America,* 101, 10554-10559.

Nakamura, T.; Kurokawa, K.; Kiyokawa, E. & Matsuda, M. (2006) Analysis of the spatio-temporal regulation of Rho GTPases using Raichu probes. *Methods in Enzomology,* 406, 315-332.

Nakamura, T. & Matsuda, M. (2009). In vivo imaging of signal transduction cascades with probes based on Forster Resonance Energy Transfer (FRET). In: *Current Protocol in Cell Biology,* Bonifacino, J. S.; Dasso, M.; Harford, J. B.; Lippincott-Schwartz, J. & Yamada, K. M., 45, Chapter 14, Unit14.10. 1-14. John Wiley & Sons, 9780471143031, Hoboken.

Nakaya, M.; Tanaka, M.; Okabe, Y.; Hanayama, R. & Nagata,S. (2006). Opposite effects of rho family GTPases on engulfment of apoptotic cells by macrophages. *Journal of Biological Chemistry,* 281, 8836-8842.

Nguyen, A. W. & Daugherty, P. S. (2005). Evolutionary optimization of fluorescent proteins for intracellular FRET. *Nature Biotechnology,* 23, 355-360.

Palm, G. J.; Zdanov, A.; Gaitanaris, G. A.; Stauber, R.; Pavlakis, G. N. & Wlodawer, A. (1997). The structural basis for spectral variations in green fluorescent protein. *Nature Structural Biology,* 4, 361-365.

Patino-Lopez, G.; Dong, X.; Ben-Aissa, K.; Bernot, K. M.; Itoh, T.; Fukuda, M.; Kruhlak, M. J.; Samelson, L. E. & Shaw, S. (2008). Rab35 and its GAP EPI64C in T cells regulate receptor recycling and immunological synapse formation. *Journal of Biological Chemistry,* 283, 18323-18330.

Periasamy, A. & Day, R. N. (1999). Visualizing protein interactions in living cells using digitized GFP imaging and FRET microscopy. *Methods in Cell Biology,* 58, 293-314.

Pertz, O.; Hodgson, L.; Klemke, R. L. & Hahn, K. M. (2006). Spatiotemporal dynamics of RhoA activity in migrating cells. Nature, 440, 1069-1072.

Pollok, B. A. & Heim, R. (1999). Using GFP in FRET-based applications. Trends in Cell Biology, 9, 57-60.

Saltiel, A. R. & Pessin, J. E. (2002). Insulin signaling pathways in time and space. *Trends in Cell Biology,* 12, 65-71.

Sako, Y. (2006). Imaging single molecules in living cells for systems biology. *Molecular Systtems Biology,* 2, 56-61.

Sato, M.; Sato, K.; Liou, W.; Pant, S.; Harada, A. & Grant, B. D. (2008). Regulation of endocytic recycling by C. elegans Rab35 and its regulator RME-4, a coated-pit protein. *EMBO Journal*, 27, 1183-1196.

Sekar, R. B. & Periasamy, A. (2003). Fluorescence resonance energy transfer (FRET) microscopy imaging of live cell protein localizations. *Journal of Cell Biology,* 160, 629-633.

Stenmark, H. (2009). Rab GTPases as coordinators of vesicle traffic. *Nature Reviewes Moelcular Cell Biology,* 10, 513-525.

Takaya, A.; Ohba, Y.; Kurokawa, K. & Matsuda M. (2007). R-Ras regulates exocytosis by Rgl2/Rlf-mediated activation of RalA on endosomes. *Molecular Biology of the Cell* 18, 1850-1860.

Takaya, A.; Ohba, Y.; Kurokawa, K. & Matsuda, M. (2004). RalA activation at nascent lamellipodia of epidermal growth factor-stimulated Cos7 cells and migrating Madin-Darby canine kidney cells. *Molecular Biology of the Cell* 15, 2549-2557.

Tsien, R. Y. & Miyawaki, A. (1998). Seeing the machinery of live cells. *Science,* 280, 1954-1955.

Tsuboi, T.; McMahon, H. T. & Rutter, G. A. (2004). Mechanisms of Dense Core Vesicle Recapture following "Kiss and Run" ("Cavicapture") Exocytosis in Insulin-secreting Cells. *Journal of Biological Chemistry,* 279, 47115-47124.

Walseng, E.; Bakke, O. & Roche, P. A. (2008). Major histocompatibility complex class II-peptide complexes internalize using a clathrin- and dynamin-independent endocytosis pathway. *Journal of Biological Chemistry,* 283, 14717-14727.

Yoshizaki, H;, Ohba, Y.; Kurokawa, K.; Itoh, R. E.; Nakamura, T.; Mochizuki, N.; Nagashima, K. & Matsuda, M. (2003). Activity of Rho-family G proteins during cell divison as visualized with FRET-based probes. *Journal of Cell Biology*, 162, 223-232.

Yuseff, M. I., Lankar, D. & Lennon-Duménil, A. M. (2009) Dynamics of membrane trafficking downstream of B and T cell receptor engagement: impact on immune synapses. *Traffic,* 10, 629-636.

Zerial, M. & McBride, H. (2001). Rab proteins as membrane organizers. *Nature Review of Molecular and Cellular Biology,* 2, 107-117.

Zhang, J.; Fonovic, M.; Suyama, K.; Bogyo, M. & Scott, M. P. (2009). Rab35 controls actin bundling by recruiting fascin as an effector protein. *Science,* 325, 1250-1254.

Zhu, A. X.; Zhao, Y. & Flier, J. S. (1994). Molecular cloning of two small GTP-binding proteins from human skeletal muscle. *Biochemica Biophysica Research Communications,* 205, 1875-1882.

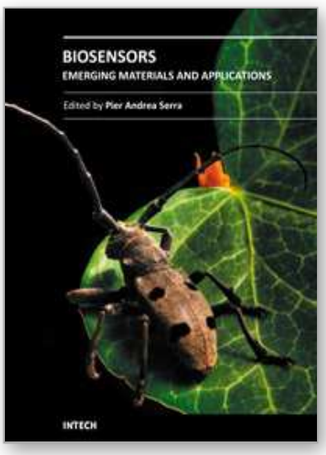

Biosensors - Emerging Materials and Applications

Edited by Prof. Pier Andrea Serra

ISBN 978-953-307-328-6
Hard cover, 630 pages
Publisher InTech
Published online 18, July, 2011
Published in print edition July, 2011

A biosensor is a detecting device that combines a transducer with a biologically sensitive and selective component. Biosensors can measure compounds present in the environment, chemical processes, food and human body at low cost if compared with traditional analytical techniques. This book covers a wide range of aspects and issues related to biosensor technology, bringing together researchers from 19 different countries. The book consists of 27 chapters written by 106 authors and divided in three sections: Biosensors Technology and Materials, Biosensors for Health and Biosensors for Environment and Biosecurity.

How to reference

In order to correctly reference this scholarly work, feel free to copy and paste the following:

Nanako Ishido, Hotaka Kobayashi, Yasushi Sako, Takao Arai, Mistunori Fukuda and Takeshi Nakamura (2011). How to make FRET biosensors for Rab family GTPases, Biosensors - Emerging Materials and Applications, Prof. Pier Andrea Serra (Ed.), ISBN: 978-953-307-328-6, InTech, Available from: http://www.intechopen.com/books/biosensors-emerging-materials-and-applications/how-to-make-fret-biosensors-for-rab-family-gtpases

INTECH
open science | open minds

InTech Europe
University Campus STeP Ri
Slavka Krautzeka 83/A
51000 Rijeka, Croatia
Phone: +385 (51) 770 447
Fax: +385 (51) 686 166
www.intechopen.com

InTech China
Unit 405, Office Block, Hotel Equatorial Shanghai
No.65, Yan An Road (West), Shanghai, 200040, China
中国上海市延安西路65号上海国际贵都大饭店办公楼405单元
Phone: +86-21-62489820
Fax: +86-21-62489821

IntechOpen